IL NUOVO CIMENTO **43 C** (2020) 25
DOI 10.1393/ncc/i2020-20025-4

Colloquia: IFAE 2019

Precision measurement of cosmic-ray nuclei with the alpha magnetic spectrometer on the International Space Station

Federico Donnini

INFN, Sezione di Roma Tor Vergata, SSDC-ASI - Rome, Italy

received 8 June 2020

Summary. — The measurement of the nuclei component in cosmic rays (CR) provides a detailed knowledge of the origin and propagation of cosmic rays. AMS-02 is a magnetic spectrometer designed to perform precision measurment of the composition and energy spectrum of cosmic rays from GeV to TeV. Using its large acceptance and long exposure time, AMS-02 is able to measure the fluxes of CR species at least up to iron, studying also the detailed variation of their spectral index as a function of the rigidity. AMS-02 was installed onboard the International Space Station on May 19, 2011 and has been continuously taking data since then. In 8 years of operations, it collected over 135 billion of cosmic-ray triggers, both primary and secondary. Primary cosmic rays, such as H, He, C, N and O, are mainly produced and accelerated by supernova explosions, while secondary cosmic rays, such as Li, Be and B are produced through collisions of heavier nuclei with the interstellar medium. In this contribution, the published results regarding the nuclear component of CR from hydrogen to oxygen, for rigidity interval between 2 GV and 3.3 TV, have been presented. The contribution will also show the preliminary measurement of the temporal evolution of carbon and oxygen fluxes, during the period between May 2011 and May 2018. This measurerement can provide important information about the propagation of CR inside the heliosphere.

1. – Introduction

Cosmic rays (CR) are charged particles continuously reaching the Earth from the outer space: about 99% of them are nuclei, the remaining are electrons with a small component (<0.1%) of anti-particles (positrons, antiprotons).

The CR energy spectrum extends from few MeVs up to 10^{20} eV: different astrophysical sources and acceleration processes contribute to the flux in different regions of the spectrum, which is also shaped by interactions of CR with the interstellar medium (ISM) and the heliosphere in the long journey from sources to Earth.

In the energy range accessible to direct measurements, CRs are thought to be accelerated by shock waves produced by supernovae explosions in our Galaxy. Elements such

as hydrogen, helium, carbon, nitrogen and oxygen, which are directly accelerated at the source, are also called primary CRs. During their propagation in the Galaxy, primary CRs are diffused by irregularities of the galactic magnetic field and interact with the interstellar medium, producing other elements, called secondary CRs, such as lithium, beryllium and boron. The secondary component of CRs is sensitive to the details of the CR propagation: the abundances and energy spectra of secondary CRs can be used to constrain the models describing the diffusion, convection or reaccelerating processes in the Galaxy. Carbon and oxygen, instead, being a primary component of CR, carry information about the sources and the acceleration mechanisms of CR. Hydrogen and nitrogen fluxes are peculiar in this scenario, since they have both a primary and a secondary component. In this paper, CR fluxes from hydrogen to oxygen, using 5 years of data collected by AMS-02 will be presented. For carbon and oxygen, a detailed temporal evolution of their energy spectra will be also discussed.

2. – Detector

AMS-02 is a large-acceptance high-energy magnetic spectrometer able to perform precision measurements of particles in the GeV–TeV energy range. The AMS-02 apparatus is composed by different sub-detectors for a complete reconstruction of the particle identity. The core of the detector is the silicon tracker, composed by 9 layers of of double-sided microstrip silicon sensors, 6 of which (L3 to L8) inside the magnetic field generated by a permanent magnet. The tracker accurately measures the curvature of particles in the magnetic field, and it allows to derive the rigidity ($R = pc/Ze$) of charged cosmic rays, with a maximum detectable rigidity (MDR) over 3 TV. Each layer of the tracker provides also an independent measurement of the charge Z with a resolution of $\Delta Z/Z$ from 4% to 9% depending on the nuclei specie. Overall, the inner tracker has a resolution of $\Delta Z/Z$ from 1.5% to 3.5%. Two pairs of plastic scintillators, placed at both ends of the tracker, measure the Time of Flight (ToF) of the particle and provide the trigger for the rest of the experiment. An anti-coincidence scintillator system (ACC) gives the veto signal in the trigger for particles entering the apparatus out of the tracker acceptance, *i.e.*, at large angles or from the sides. The AMS-02 detector is completed by other three sub-detectors which provide the particle identification capabilities: a Ring Image Cherenkov (RICH) below the magnet to measure of the particle velocity; the Transition Radiation Detector (TRD) placed on top of AMS-02 and an Electromagnetic Calorimeter (ECAL) at the bottom for the accurate distinction between leptons and hadrons. More details on the various sub-detectors can be found in [1] and references therein.

3. – Event selection

The AMS-02 detector, with its large acceptance and long exposure time, is able to perform precision measurement of the hadronic component in CRs for nuclei up to Fe (fig. 1(left)). In the first 5 years (May the 19th, 2011 to May the 26th, 2016) AMS-02 has collected $8.5 \cdot 10^{10}$ cosmic-ray events. The collection time includes only those seconds during which the detector was in normal operating conditions, AMS-02 was pointing within 40° of the local zenith, and the ISS was outside of the South Atlantic Anomaly. The measured rigidity is also required to be greater than 1.2 times the maximum geomagnetic cutoff within the AMS field of view. The cutoff was calculated by backtracing [2] particles from the top of AMS out to 50 Earth's radii using the most recent IGRF geomagnetic model [3].

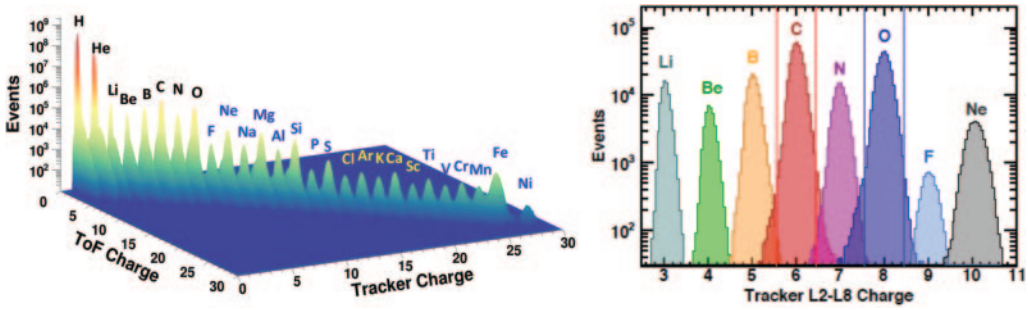

Fig. 1. – Left: charge measurement provided by the inner tracker and ToF; AMS-02 is able to perform precise measurement of the hadronic component in CRs for nuclei up to Fe. Right: charge distribution measured by the inner tracker (L2–L8) for samples from $Z = 3$ to $Z = 10$ selected by the combined charge measured with L1, the upper TOF, and the lower TOF over the rigidities above 4 GV. The colored vertical lines show as example the charge selection applyed in the inner tracker for carbon (red) and oxygen (blue).

The identification of each nuclei specie is achieved by applying charge selections on the tracker L1, inner tracker, upper TOF and, for highest rigidities (>1 TV), tracker L9 (fig. 1(right)). Additional information on the event selection can be found in ref. [4].

The residual background for the event samples have two sources. The first one comes from the interaction of heavier nuclei in the material between L1 and L2 (TRD and upper TOF). Since hydrogen is the dominant component of cosmic rays, the selected sample has negligible contributions of other particles. For higher nuclei, instead, this residual background is evaluated by fitting the charge distribution of tracker L1 with charge distribution templates of Li, Be, B, C, N and O as shown in fig. 2. The templates are obtained from samples selected to be non-interacting samples at L2 by the use of the charge measurement with L1 and L3–L8. This background is found to be <0.5% for Li, Be and C, <3% for B, <5% for N and negligible for O, over the entire rigidity range.

The second source of background comes from nuclei interacting in materials above L1 (thin support structures made of carbon fiber and aluminum honeycomb). It has been estimated from simulation using MC samples generated according to AMS flux measurements. This background is <0.5% for H and C and negligible for He and O over the entire rigidity range; for Li, Be, and B this background is 5%, 8%, and 5% at 2 GV and 2%, 3%, and 8% at 3.3 TV, respectively; the background for nitrogen, instead, is 3% below 200 GV and 6% at 3.3.

4. – Data analysis

The isotropic flux Φ_i in the i-th rigidity bin $(R_i, R_i + \Delta R_i)$ is given by

$$\Phi_i = \frac{N_i}{A_i \epsilon_i T_i \Delta R_i}, \tag{1}$$

where N_i is the number of events of a given nuclei specie, corrected for bin-to-bin migrations, A_i is the effective acceptance, ϵ_i is the trigger efficiency, and T_i is the collection time.

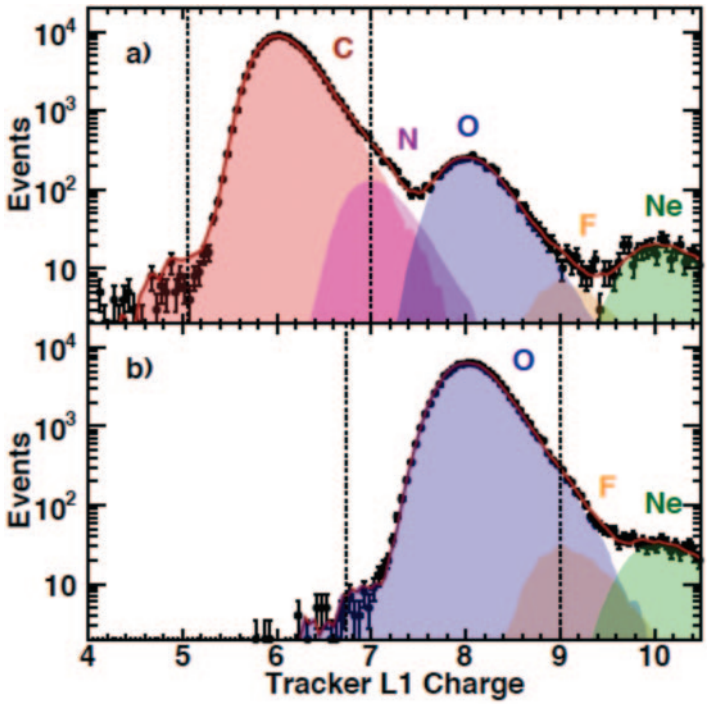

Fig. 2. – Charge distributions measured by tracker L1 for (a) carbon and (b) oxygen events selected by the inner tracker in the rigidity range between 9 and 11 GV (black dots). The solid red curves show the data of the C, N, O, F, and Ne charge distribution templates. The charge selections applied on tracker L1 are shown as vertical dashed lines. The residual backgrounds to the carbon and oxygen samples are calculated by integrating the charge template distributions over the selection range.

The bin-to-bin migration of events was corrected using the unfolding procedure described in ref. [5] independently for the helium, carbon, and oxygen samples.

The trigger efficiency for hydrogen ranges from 90% to 95%. The 5% to 10% inefficiency is due to secondary δ rays in the magnetic field entering the ACC. For other nuclei, instead, the trigger efficiencies have been measured to be: >94% for helium and >97% for nuclei with $Z > 2$ over the entire rigidity range. A detailed description of the trigger efficiency evaluation can be found in ref. [6].

The detector acceptance directly relates the number of selected particles to the flux and depends on the detector geometry as well as on the detection and selection efficiencies. The acceptance of AMS-02 has been evaluated using a Monte Carlo (MC) simulation of the entire detector, since an analytical calculation is impractical even for simple detector geometries and neglecting efficiency effects.

The AMS-02 Monte Carlo simulation, based on the GEANT-4.10.1 package [7], contains a detailed description of the detector: its geometry and its composition, with the best possible estimates of the matter density distribution of both active and passive areas in the instrument. The detector description is combined with a simulation of the physical processes that take place inside the detector when a charged particle passes through.

Once the various energy depositions and interactions of particles inside the detector are described, the hit simulation produces the experimental signals which set the basis for an event reconstruction, performed in the same way as for the real data. The end result is a data structure similar to the one obtained in the flight data. The simulation is validated comparing the reconstruction and selection efficiencies estimated from flight data with those obtained from the simulation itself: any difference between the two evaluations of each efficiency is used to correct the estimated acceptance and to assess the systematic uncertainty on the measurement.

The contributions to the systematic errors come from the uncertainties in the two background estimations and the trigger efficiency, the geomagnetic cutoff factor, the acceptance calculation, the rigidity resolution function and the absolute rigidity scale.

5. – Results

The measured fluxes, as shown in fig. 3(left), clearly show an hardening of the spectrum above 200 GV, which can be described as a smooth transition of the spectral index.

In order to better examine the rigidity dependence of the fluxes, the variations of their spectral indices with rigidity has been evaluated. The flux spectral index is calculated from

$$\gamma = \mathrm{d}[\log(\Phi)]/\mathrm{d}[\log(R)], \tag{2}$$

over non-overlapping rigidity intervals above 8.48 GV, with a variable width to have sufficient sensitivity to determine γ. As a result, the magnitude and the rigidities dependence of the helium, carbon, and oxygen spectral indices are very similar. In particular, all spectral indices are identical within the measurement errors above 60 GV and all spectral indices harden with rigidity above 200 GV (fig. 3(right)).

Figure 3 shows also that the three secondary fluxes have identical rigidity dependence above 30 GV as do the three primary fluxes above 60 GV, but they are different from each other. The rigidity dependences of the nitrogen and hydrogen fluxes are distinctly different from the dependence of both the primary fluxes and the dependence of the secondary fluxes.

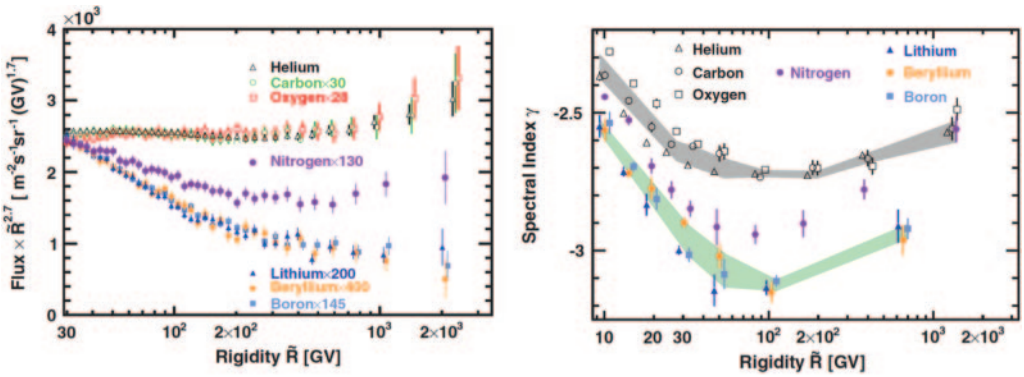

Fig. 3. – Left: comparison of the AMS measurements of nucle fluxes up to oxygen. For display purposes, the C, O, Li, Be, B, and N fluxes were rescaled as indicated. Right: the rigidity dependence of the spectral indices of nuclei up to oxygen.

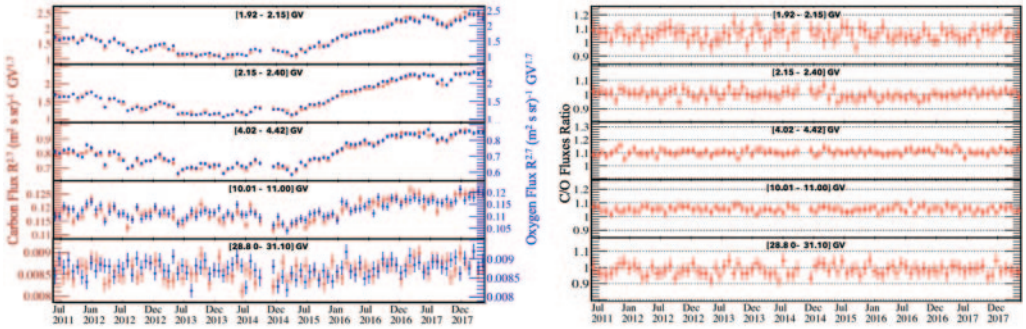

Fig. 4. – Left: the AMS carbon (red, left axis) and oxygen (blue, right axis) fluxes multiplied by $R^{2.7}$ with the statistical uncertainties, as a function of time from May 2011 up to May 2018, for 5 rigidity bins. Right: the AMS C/O ratio with the statistical uncertainties, as a function of time from May 2011 up to May 2018.

6. – Time variation

AMS is also able to measure the time evolution of the nuclei fluxes. The fluxes have been evaluated according to eq. (1), in the time interval of a Bartels rotation, which corresponds to 27 days. Additional information regarding how the time behavior measurement is performed can be found in [8]. Figure 4(left) shows the preliminary measurement of the C and O fluxes behavior up to May 2017 for 5 characteristic rigidity intervals. Both the C and O fluxes, as seen for p and He [8], exhibit large variations with time at low rigidities which decrease with increasing rigidity and vanish above 30 GV. The time behavior of the C and O fluxes is similar; this is confirmed in fig. 4(right), which shows the costant time behavior of the C/O ratio for the 5 characteristic rigidity bins.

In order to better understand these behaviors, great effort to reduce the statistical fluctuations on the C and O fluxes is still ongoing.

7. – Conclusions

A detailed knowledge of the nuclei fluxes in cosmic rays and their time evolution is important in understanding the origin, acceleration, and propagation of cosmic rays. The precise measurement of the nuclei fluxes from hydorgen to oxygen, from 2 GV to 3.3 TV provided by AMS-02 has been presented. The results show that the three secondary fluxes have identical rigidity dependence above 30 GV as do the three primary fluxes above 60 GV, but they are different from each other. The rigidity dependence of the nitrogen and the hydrogen fluxes is distinctly different from the dependence of both the primary fluxes and the dependence of the secondary fluxes.

REFERENCES

[1] Aguilar M. *et al.*, *Phys. Rev. Lett.*, **110** (2013) 141102.
[2] Alcaraz J. *et al.*, *Phys. Lett., B*, **183** (2016) 1216.
[3] Finlay C. *et al.*, *Geophys. J. Int.*, **484** (2000) 10.
[4] Aguilar M. *et al.*, *Phys. Rev. Lett.*, **119** (2017) 251101.

[5] AGUILAR M. *et al.*, *Phys. Rev. Lett*, **114** (2015) 171103.
[6] AGUILAR M. *et al.*, *Phys. Rev. Lett.*, **115** (2015) 211101.
[7] ALLISON J. *et al.*, *Nucl. Instrum. Methods Phys. Res., Sect. A*, **835** (2016) 186; AGOSTINELLI S. *et al.*, *Nucl. Instrum. Methods Phys. Res., Sect. A*, **506** (2003) 250.
[8] AGUILAR M. *et al.*, *Phys. Rev. Lett.*, **121** (2018) 051101.